

Flattening Scientific CCD Imaging Data with a Dome Flat Field System

J. L. Marshall & D. L. DePoy

Department of Astronomy, The Ohio State University

140 West 18th Avenue, Columbus, Ohio 43210-1173

marshall@astronomy.ohio-state.edu, depoy@astronomy.ohio-state.edu

ABSTRACT

We describe the flattening of scientific CCD imaging data using a dome flat field system. The system uses light emitting diodes (LEDs) to illuminate a carefully constructed dome flat field screen. LEDs have several advantages over more traditional illumination sources: they are available in a wide range of output wavelengths, are inexpensive, have a very long source lifetime, and are straightforward to control digitally. The circular dome screen is made of a material with Lambertian scattering properties that efficiently reflects light of a wide range of wavelengths and incident angles. We compare flat fields obtained using this new system with two types of traditionally-constructed flat fields: twilight sky flats and nighttime sky flats. Using photometric standard stars as illumination sources, we test the quality of each flat field by applying it to a set of standard star observations. We find that the dome flat field system produces flat fields that are superior to twilight or nighttime sky flats, particularly for photometric calibration. We note that a ratio of the twilight sky flat to the nighttime sky flat is flat to within the expected uncertainty; but since both of these flat fields are inferior to the dome flat, this common test is not an appropriate metric for testing a flat field. Rather, the only feasible and correct method for determining the appropriateness of a flat field is to use standard stars to measure the reproducibility of known magnitudes across the detector.

Subject headings: instrumentation: detectors, techniques: imaging processing, techniques: photometric

1. Introduction

Charge-coupled devices (CCDs) and other modern array detectors dominate optical and near-infrared observations in astronomy: as of this writing there are nearly 6000 papers in refereed journals with “CCD” in their titles or abstracts and many more include infrared array data. The primary reason for this ubiquity is that these detectors are nearly perfect for astronomical observations. They detect photons with high efficiency and produce an electronic signal capable of easy assimilation into digital recording, which has many subsequent advantages for data reduction and

analysis. They also typically impose very little (often no significant) additional noise onto the observations. McLean (2002) summarizes and discusses the history and advantages of array detectors in astronomy. New varieties of detectors are on the horizon (e.g. Rando et al. 2000), but CCDs and near-infrared arrays seem likely to continue to dominate ground-based optical and near-infrared observations for many years.

CCDs and similar detectors have several characteristics that impose systematic signatures on any data they collect. The CCD’s “bias” is a constant signal present in the absence of photons and independent of exposure time. “Dark current” is not produced by photons, but does increase with exposure time. Some CCDs may not be very “flat,” i.e., they may have differences in the response to photons by the individual pixels of the detector (although modern CCDs in particular can be very flat; see Morgan et al. 2005, for an example) and may require division by a “flat field” to remove these differences. Accurate interpretation of the data requires that these artifacts be removed during the reduction and analysis process. Bias and dark current are typically accounted for with special images taken without illumination of the detector, obtained under otherwise identical conditions (exposure time, device temperature, etc.) or with special electronic images obtained to mimic the signal present in a pixel without light (often added to the data frame and called an “overscan” region). There are other characteristics that can also affect data quality (non-linear response, charge transfer efficiency, residual signal, fringing, shutter timing, etc.), although these tend to be minor in modern detectors and for most applications (see Mackay 1986; McLean 1994, for additional discussion).

Unlike bias and dark current subtraction, flat field correction requires exposure to light and should reproduce the illumination of the science observations onto the detector. An ideal flat field removes the small response differences between pixels of the detector as well as field-dependent non-uniformities in the throughput of the optics. Unfortunately, a perfect flat field is difficult to obtain in practice for at least two reasons. First, the detector must be illuminated in a manner that exactly replicates the illumination pattern of the actual observations. Necessarily this means that the pupil of the optics must be accurately reproduced or that the actual pupil must be evenly illuminated. The pupil can be defined as the largest optical surface that intercepts all angles from the observed field and is typically the primary mirror of the telescope (although not always; see Zhou et al. 2004). Achieving constant illumination over a large optic is challenging, particularly in the presence of scattered light (see Grundahl & Sorenson 1996; Kuhn & Hawley 1999). Second, the flatness of any detector depends on the spectrum of the incident light (Mackay 1986). Therefore, the illumination source must reproduce the color of the light that is to be detected. Reproducing this spectrum is generally impossible, since on any given image different sources have different spectra and the sky will contribute a variable amount depending on the relative brightness of the source. The magnitude of the effect of a color mismatch between flat fields and observations when applying flat fields to CCD observations varies from detector to detector and is often not well measured.

There are three common methods of obtaining a flat field. Most typically, images are obtained of either the bright twilight sky (“sky flats”) or of a nearby screen placed in front of the telescope

that is illuminated by projected light (“dome flats”). Occasionally a flat field is made from the combination of many images taken of the nighttime sky. There are positive and negative aspects to each of these techniques. For example, twilight sky flats must be obtained at a relatively restricted range of times after sunset (see Tyson & Gal 1993) and can have significant gradients in illumination (particularly for wide field observations; see Chromey & Hasselbacher 1996). In practice, it is often difficult to obtain all necessary calibration images in the relatively short time available during twilight (particularly for inexperienced observers). Dome flats are convenient to obtain and can have very high signal-to-noise (S/N), which reduces noise added to the science image by the data reduction process (see Newberry 1991). However, the color and pattern of the illumination may not reproduce the observations well. The presence of illumination sources not present during the actual observations (i.e. scattered light from the telescope or dome) can compromise the accuracy of all these techniques (see Manfroid et al 2001, for example). Nighttime sky flats have other complications, mainly that it is difficult to obtain high enough S/N for most applications. Other techniques for obtaining flat fields have been introduced: multiple exposures of time-independent signals at different spatial positions on the detector (Kuhn, Lin, & Lorz 1991; Toussaint et al 2003), scanning extended sources (Dalrymple et al 2003), dithered observations of non-uniform background sources (Wild 1997), and simultaneous observation of many photometrically-calibrated stars (Manfroid 1995, 1996), for example. Most of these techniques have not been widely adopted at nighttime-oriented observatories.

In this paper we describe a dome flat field system that uses a specially constructed screen and banks of modern light emitting diodes (LEDs) as illumination sources. LEDs offer significant advantages over more traditional sources of illumination and allow for the potential of greater flat field accuracy and improved photometric performance. We find that carefully constructed dome flats outperform twilight or nighttime sky flats for photometric calibration of CCD images.

2. Description of Dome Flat Field System

Below we describe the two primary components of the dome flat field system installed at the McGraw-Hill 1.3 m telescope at the MDM Observatory (<http://www.astro.lsa.umich.edu/obs/mdm/>). The system consists of a screen and a set of illumination sources. The screen is similar to that installed at many observatories, but it is nonetheless a crucial component of the system so we include a description of its properties. The illumination system is a set of LEDs that ring the top end of the telescope.

2.1. Flat Field Screen

The flat field screen is a special piece of equipment; it is not simply a white sheet draped against the dome wall. The screen is circular in shape, stretched tightly onto a metal ring to minimize

wrinkles and shadows. The screen is attached to the interior of the dome and mounted face-on to the secondary ring of the telescope. Ideally, the screen should be perpendicular to the optical axis of the telescope so that it best fills the aperture of the telescope and provides the most predictable reflectance pattern into the telescope beam. In practice, this geometry is often difficult to obtain due to the mismatch between the locations of the center of rotation of the dome and telescope axes. In Section 3 we discuss the differences between dome flats taken at a variety of telescope pointing and dome rotation combinations.

The screen consists of white fabric surrounded by a wide annulus of black fabric. Figure 1 shows a picture of the screen mounted on the inside of the dome at the McGraw-Hill 1.3 m telescope. The diameter of the white area is 1.3 m; the surrounding black fabric is an annulus roughly 0.6 m in width. The white spot is the same diameter as the primary mirror of the telescope so that it fills the pupil of the telescope well (but does not overfill it and thereby introduce extraneous off-axis illumination). The black material surrounding the reflective spot is essential in reducing scattered light onto the primary mirror (see Grundahl & Sorenson 1996, for a discussion of scattered light issues).

The flat field screen was manufactured by Stellar Optics Research International Corporation of Thornhill, Ontario, Canada (<http://www.soric.com>). It is made of a durable “SORICSCREEN” fabric with high and relatively constant reflectance from the ultraviolet to the near-infrared. The screen has Lambertian scattering properties at a wide range of incident angles. Figure 2 shows the reflectance of the material versus wavelength, which varies only by $\sim 2\%$ from 350 nm to 1000 nm. The material used for the white spot is more fully described by McCall & Siegmund (1994).

We note that this screen design is similar to that in use at the Cerro Tololo Inter-American Observatory (CTIO) at the Blanco 4 m telescope and other smaller telescopes. This system has worked well for many years.

2.2. Illumination Sources

Light emitting diodes (LEDs) are very popular semiconductor devices that are found in an amazing variety of applications (e.g. flashlights, automobile taillights, supermarket scanners, and stadium picture displays). They are inexpensive (\$0.01 to \$10.00) and have extremely long lifetimes ($\sim 100,000$ hours, depending on operating conditions). Furthermore, they can be controlled by simple digital electronics and require only low voltage for operation (typically 3-10 V). LEDs with very high brightness and an extremely wide range of colors have recently been developed. As an example, Figure 3 shows the relative spectral energy distribution of the output light of a number of LEDs from one particular manufacturer (Ledtronics, Inc.; see <http://www.ledtronics.com>). There are many more LED manufacturers; for example, Roithner-Lazertechnik (<http://www.roithner-laser.com>) has a good selection of far red LEDs that complement the bluer LEDs shown in Figure 3. The combination of these characteristics suggest that LEDs make an excellent choice for flat field

illumination sources.

We selected five LEDs corresponding with each of the optical bandpasses (i.e., U, B, V, R, and I) in use at the telescope. Each LED was chosen so that the central wavelength was close to the center of the traditional UBVRI filters and with significant emission over most of the bandpass. We refer to the LEDs by the bandpass with which they are associated. We note that, to the eye, the color of the illumination looked approximately white with all the LEDs turned on. In general, the LEDs have relatively wide projection angles in order to illuminate the flat field screen fully. Table 1 gives details of the specific LEDs we used. Figure 4 shows the spectral energy distribution of the light output of some of the LEDs used along with the filter bandpasses (note that the brightness and peak output wavelength varies with temperature: $\sim 1\%/^{\circ}\text{C}$ in brightness and $\sim 0.1\text{ nm}/^{\circ}\text{C}$ in wavelength are typical). Again we emphasize that there are a wide variety of LEDs available with various colors; many combinations are possible that will suit other applications. The LEDs are attached to the top of the secondary ring of the telescope. One LED of each of the five colors is mounted at each of the cardinal points of the ring.

The most important consideration for the flat field screen illumination system is the uniformity of the radiance (radiant power from a given direction per unit area of the source per unit solid angle) of the screen as viewed from the focal plane of the telescope: the illumination of the focal plane must be uniform over the area of the field of view as well as the range of solid angles of incident light. We note that our screen is not very evenly illuminated (i.e., the screen looks mottled). While the illumination pattern on the screen does not appear very smooth to the eye, in fact, the combination of the scattering effects of the screen and the effects of the telescope optics produces a relatively uniformly illuminated field of view at the focal plane. We demonstrate the uniformity of the radiance of our dome flat field system explicitly in Section 3.

3. Characterization of Performance of Flat Fields

3.1. Construction of the Flat Fields

We obtained twilight sky flats, dome flats, and nighttime sky flats at the MDM 1.3m telescope. Twilight sky flats were obtained in the usual manner (see Tyson & Gal 1993) during evening twilight under clear conditions. We obtained dome flats at three different combinations of telescope pointing and dome position. These were 60 second exposures. We also created a flat field from ~ 75 long exposures of the nighttime sky. A large number of exposures were obtained to create each flat: approximately 20 images at each dome flat position, and 10 images of the twilight sky during one twilight period. The typical signal was 15000-25000 electrons per pixel above the detector bias level in each twilight sky and dome flat image, ensuring excellent formal S/N in each combined flat ($S/N \sim 400$). The bias and any small dark signal was removed from the images prior to combination

into each final flat using standard IRAF¹ utilities.

A 1024×1024 SITe CCD was used for all the measurements; the CCD has 0.024 mm pixels, which correspond to ~ 0.5 arcsec at the $f/7.5$ Cassegrain focus of the 1.3 m telescope. A filter wheel mounted ~ 50 mm above the CCD holds a Johnson V filter ($\lambda \approx 550$ nm; $\Delta\lambda \approx 90$ nm). All measurements were made on 21 September 2003. Care was taken to minimize effects not due to the illumination of the CCD or its intrinsic properties. For example, exposure times for all flats were sufficiently long that shutter timing effects are small (< 0.002 mag). Also, the maximum signal on the CCD was kept well below saturation and any non-linearity or charge transfer effects should be < 0.001 mag.

3.2. Direct Comparison of Flat Fields

Twilight sky flats are the most common form of flats applied to imaging data at many observatories. They are typically assumed to represent the most constant illumination of the detector and to give an image that removes the individual pixel-to-pixel variations in response and any overall illumination pattern imposed by the system optics. Of course, the observer has almost no control over the brightness or color of these flats or any scattered light and color effects that are potentially problematic.

A standard test of a twilight sky flat is to compare it to an image made from the median combination of a large number of deep nighttime sky images (i.e. essentially a deep image of the sky without any stars). It is often presumed that if the twilight sky flat makes the nighttime sky image flat and free of any large scale residuals, then it must be a good approximation of the overall illumination of the detector. The assumption is made that the illumination of the detector by the nighttime sky is uniform and without serious contaminants or significant illumination gradients.

Indeed, when we ratio the twilight sky flat to the nighttime sky flat described above we find a very uniform result. A histogram of the values in the ratio is shown in Figure 5, which has been normalized to unity for convenience. The standard deviation of the ratio is 0.7%, roughly consistent with the S/N of the two individual flats (although dominated by the S/N of the nighttime sky flats). Further, there is no large scale structure in the ratio with an amplitude greater than 0.1%. This implies that the twilight sky flat and the nighttime sky flat are essentially the same; we will use only the twilight flat (since it has higher S/N) for the remainder of this analysis.

We tested the dome flats in a similar manner, creating a ratio of each of the three dome flats to the twilight sky flat. In each case, there were obvious large scale residuals in the result. These residuals were as large as 1.5% in amplitude over ~ 100 pixel scales in the ratio; an example is shown in Figure 6. Some of the features seen in this image ratio are clearly due to dust or other

¹IRAF is distributed by the National Optical Astronomy Observatories, which is operated by the Association of Universities for Research in Astronomy, Inc., under cooperative agreement with the National Science Foundation.

debris that moved during the time between the dome flats and the twilight sky flats; this material is most likely on the filter or cryostat window, both of which are near the focal plane. Even if these features are ignored, there are other large scale structure and gradients in the ratio of the dome flats to the twilight sky flat, suggesting that there are significant differences in the illumination of the detector between these two flat fields. In Section 3.3 we discuss these differences in more detail.

The three dome flat positions comprise three different combinations of telescope pointing and dome rotation. For dome flat position #1, the telescope was pointed most directly at the flat field screen and the screen was most nearly perpendicular to the optical axis of the telescope. Dome flat position #2 was nearly as well pointed, but the telescope was pointed slightly off the center of the screen; dome flat position #3 was significantly off-center and the screen was not very perpendicular to the primary mirror.

We compared the three dome flats by forming ratios of the flats obtained at each pointing. The standard deviation of the results was $\sim 2\%$, larger than that expected from the estimated S/N of the individual flats. Indeed, there were obvious systematic features in the ratios. These included features similar to those seen in Figure 6, although of somewhat smaller amplitude ($\sim 1\%$). This suggests again that dust or other obscuring material on the optics near the detector had moved slightly as the telescope was re-positioned. There were also gradients seen in the ratios. In the case of the ratio of dome flat #1 to dome flat #3, there was a gradient of $\sim 5\%$ diagonally across the detector. A smaller gradient ($\sim 2\%$) was seen in the ratio of dome flat #1 to dome flat #2; the direction of this gradient was nearly orthogonal to that seen in the ratio of dome flat #1 to dome flat #3.

These tests would appear to suggest that the twilight sky flat is the most accurate flat; the twilight sky flat certainly seems to make the flattest and cleanest looking result when compared to the nighttime sky flat. It is possible, however, that both the twilight sky flat and the nighttime sky flat simply have the same scattered light pattern. If so, then the apparent cleanliness of their ratio does not indicate that the twilight sky represents the most accurate reproduction of the illumination of the detector by the science targets. There is no direct way to determine whether small amounts of scattered light or other inappropriate light contaminates the twilight and nighttime sky flats equally.

In general, image ratios do not contain sufficient information to properly evaluate the appropriateness of different flats. Either the ratio appears “clean” (i.e. very flat, no small or large scale artifacts) or not. If clean, then the ratio may simply indicate a common degree of contamination of the two frames. If not, then it may be impossible to tell which component of the ratio is problematic. We suspect that the twilight and nighttime sky flats are both contaminated by the same amount and pattern of scattered light and that the illumination pattern is the same in both cases.

3.3. Tests of Flat Fields Using a Grid of Standard Stars

A well-designed flat field system should produce uniform radiance of incident light at the entrance pupil of the telescope. Specifically, the flat field system should reproduce the pattern of incident light from science targets; both the spatial and angular patterns must be accurately simulated over the field of view of the detector. It is difficult to determine directly whether the system actually meets these requirements, since it would require careful, calibrated determination of the radiance of light hitting all parts of the telescope primary mirror and from all incident angles of interest coming from the flat field system. Instead, we can use the observation of many standard stars over the entire detector as a proxy for this difficult measurement. The scatter in the derived photometric zero points of the standard stars can serve as a surrogate for a measurement of the uniformity of the entrance pupil illumination and defines a good measure of the appropriateness of the flat field.

We observed a field containing the standard stars SA112-275, SA112-250, and SA112-223 (see Landolt 1992) a large number of times, moving the field center in a raster pattern between exposures. The pattern was a 12×6 grid with a spacing of approximately 1 arcminute. Figure 7 shows the positions of the standard stars over the entire set of images; roughly 75% of the detector was covered. For some of the telescope pointings only two of the standard stars were within the field-of-view of the CCD; on a few others the star fell on a bad column or pixel. For these reasons, there were a total of 205 useful measurements. All observations were made using a standard broadband Johnson V filter (the same as was used for the various flats) and had an exposure time of 5 seconds. The images were obtained at airmasses of 1.177 to 1.202. The night was clear and photometric, so the expected change in the extinction over the period of the observations is <0.002 mag.

The images of the standard stars were reduced in the usual manner using IRAF utilities, which consisted of overscan subtraction and application of a flat field. We compared four different flat fields applied to our data: a typical twilight sky flat and the three different dome flats described above. We also applied no flat field to the images (i.e. only the bias was subtracted from the images of the standard stars) to provide a baseline reference for the flats.

We derived photometric zero points from aperture photometry taken from all of the reduced images. A 12 arcsec aperture was used to measure each star; the sky was estimated in an annulus of 16 to 24 arcsec in diameter around each star. The seeing during the observations of the standard stars was ~ 1.5 arcsec. Seeing variations were $<5\%$ over the course of all the measurements, which should ensure that aperture related effects (i.e. a variable amount of the stellar signal falling out of the aperture) are <0.001 mag. Note that the colors of the three standard stars are very different ($B - V = 0.45-1.21$). Since the combination of our filter and detector are not identical to the instrumentation used to determine the standard star magnitudes (see Landolt 1992), there is a color-dependent term that affects the absolute value of the derived zero point. This effect was clearly detected in our measurements; it was removed assuming a linear relation.

To compare the relative quality of each of our five flat fields, we first simply derive the photometric zero point of each standard star as a baseline measurement. Table 2 shows the sample standard deviation of the zero point determination from each set of flattened images, including the set that had no flat field applied. Column 1 of Table 2 shows the standard deviation of all 205 determinations of the zero point for each of the sets of images. In all cases applying a flat field reduces the standard deviation; none of the flats seems to make the determination of the zero point less accurate than doing nothing. The smallest standard deviation is $\sim 0.66\%$; this result was obtained using the dome flat in position #1. For comparison, using a twilight sky flat gave a standard deviation in the zero point determination of $\sim 0.93\%$: better than applying no flat at all, but worse than dome flat positions #1 and #2.

A formal calculation of the expected signal from the stars suggests the standard deviation should be ~ 0.002 mag (if the flat fields had infinite S/N and perfectly reproduced the telescope pupil). We suspect the difference between the theoretical standard deviation and what we measure is due to a combination of small effects: small instability in shutter timing, small photometric variations, and uncertainties in the brightness of stars.

In an effort to find scattered light effects in any of the flat fields, we next fit various gradients to the photometric zero points and subtracted these small slopes from the data. Columns 2-6 of Table 2 give these results as standard deviations of the zero points after this subtraction. We fit horizontal and vertical gradients, as well as gradients radiating from the center of the CCD and diagonal gradients from upper left to lower right and lower left to upper right. Each of these applied gradients makes an improvement in at least one of the flat fields. Note in particular that the twilight sky flat is improved significantly (~ 0.003 mag) by removal of a horizontal gradient.

Dome flat position #1 is least affected by removal of any gradient. For each of the gradients considered, the change in the standard deviation of the zero points is very small for dome flat #1, typically $\lesssim 0.001$ mag. This suggests that dome flat #1 has very good angular uniformity of illumination and is therefore the best flat field. Dome flat position #2 is nearly as good as #1. Dome flat position #3, which is pointed significantly off the center of the flat field screen, has significant gradient effects and is not as good a flat field as the previous two, demonstrating the importance of aligning the telescope and dome flat field screen in creating the flats.

The very best flat field we obtained is the twilight sky flat after removal of the horizontal gradient. In fact, the horizontal gradient seen in Figure 6 can now be explained, and is wholly due to the twilight sky flat since the dome flat exhibits no gradient at all. It should be noted, however, that without the detailed analysis of hundreds of standard stars placed across the entire detector it would have been impossible to detect and remove this gradient. For all practical purposes, dome flat position #1 is the best flat field presented here.

We conclude that dome flat position #1 is the best flat field for determination of photometric zero points. This suggests it represents the most even illumination of the telescope pupil and does an adequate job of removing pixel-to-pixel variations (although the test presented here averages

out these small scale variations).

4. Discussion & Conclusions

A well-constructed dome flat can have superior performance to twilight sky flats, and indeed can flatten CCD data better than a twilight sky flat. Dome flats also have several practical advantages over sky flats, most importantly that they are more easily and reliably obtained. Twilight sky flats are prone to having lower than desirable S/N , especially if the observer is inexperienced or the run is short; in particular, it is difficult to obtain sky flats of many colors in one twilight period. Twilight flats are influenced by the presence of clouds in the field even though certain nighttime observing programs may not be. Dome flats clearly have an advantage over sky flats in all these regards. Dome flats may be obtained at any time of the day, given a sufficiently dark dome environment. They are very reproducible, and once one is assured that the dome flat is indeed superior to a sky flat a dome flat field will be equally good night after night. Very high S/N dome flats are straightforward to obtain by integrating as long as necessary and by taking a very large number of exposures. These exposures may be obtained during the day to facilitate long integrations as well as any and all bandpasses to be observed each night.

LEDs are an ideal illumination source for dome flat fields. They are available in a wide range of colors and beam patterns; it is straightforward to combine a selection of LEDs to illuminate a flat field screen of any size and in any bandpass. In particular, LEDs of different colors can be combined to produce a flat field of almost any arbitrary color. LEDs are inexpensive and bright; not many units are required to illuminate a large screen. They are easy to use and to control with simple electronics, and do not have the time-variability issues associated with incandescent illumination sources. Long lifetimes minimize time between replacement and thereby reduce personnel commitments to maintain the system.

The matching of color between flat fields and nighttime science observations may be a factor in the construction of flat field frames, and one which we do not address here. If this is the case, various LEDs may be carefully selected to produce any spectrum desired to illuminate a dome flat field screen.

A similar system to that described here is currently in use at the CTIO/SMARTS Consortium 1.3m telescope in Chile. The system at this telescope also uses an array of LEDs to illuminate a white screen.

The MDM Observatory and The Ohio State University Department of Astronomy provided support for the construction and installation of the flat field system.

REFERENCES

- Chromey, F. R. & Hasselbacher, D. A. 1996, *PASP*, 108, 944
- Dalrymple, N. E., Bianda, M., & Wiborg, P. H. 2003, *PASP*, 115, 628
- Grundahl, F. & Sorenson, A. N. 1996, *A&AS*, 116, 367
- Kuhn, J. R. & Hawley, S. L. 1999, *PASP*, 111, 601
- Kuhn, J. R., Lin, H., & Lorz, D. 1991, *PASP*, 103, 1097
- Landolt, A. U. 1992, *AJ*, 104, 340.
- Mackay, C. D. 1986, *ARA&A*, 24, 255
- Manfroid, J. 1995, *A&AS*, 113, 587
- Manfroid, J. 1996, *A&AS*, 118, 391
- Manfroid, J., Royer, P., Rauw, G., & Gosset, E. 2001, in *ASP Conf. Ser.*, Vol. 238, *Astronomical Data Analysis Software and Systems X*, eds. F. R. Harnden, Jr., F. A. Primini, & H. E. Payne (San Francisco: ASP), 373
- McCall, S. H., & Siegmund, W. A. 1994, *Proc. SPIE Vol 2198*, p. 1385-1388, *Instrumentation in Astronomy VIII*, David L. Crawford; Eric R. Craine; Eds.
- McLean, I. S. 1994, *Experimental Astronomy*, 3, 235
- McLean, I. S. 2002, *Experimental Astronomy*, 14, 25
- Morgan, C. W., et al. 2005, *AJ*, 129, 2504
- Newberry, M. V. 1991, *PASP*, 103, 122
- Rando, N., Verveer, J., Andersson, S., Verhoeve, P., Peacock, A., Reynolds, A., Perryman, M. A. C., & Favata, F. 2000, *Review of Scientific Instruments*, 71, 4582
- Toussaint, R. M., Harvey, J. W., & Toussaint, D. 2003, *AJ*, 126, 1112
- Tyson, N. D., & Gal, R. R. 1993, *AJ*, 105, 1206
- Wild, W. J. 1997, *PASP*, 109, 1269
- Zhou, X., Burstein, D., Byun, Y., Chen, W., Jiang, Z., Ma, J., Sun, W., Windhorst, R. A., Wu, H., Xu, W., & Zhu, J. 2004, *AJ*, 127, 3642



Fig. 1.— Photograph of the dome flat field screen at the McGraw-Hill 1.3m telescope. The screen is attached to a tubular ring, which is mounted to the inside of the dome. The bright line is the seam between two panels of SORICSCREEN material, and has no measurable effect on the performance of the screen. Note the relatively large area of dark material around the white spot, which serves to reduce the amount of off-axis light scattered into the telescope beam. The telescope is not pointed at the screen in this photograph.

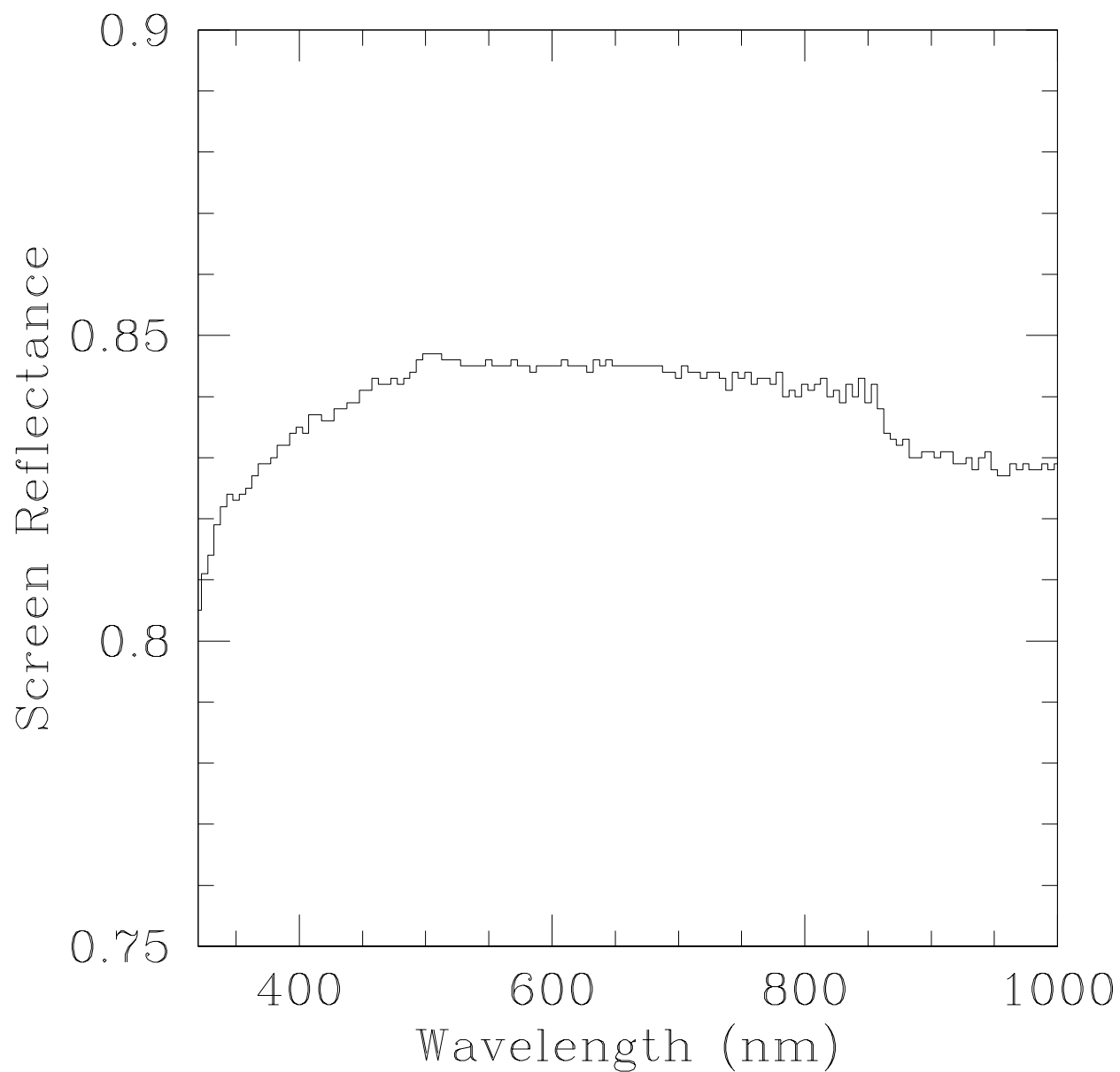


Fig. 2.— Reflectance of SORICSCREEN material in the ultraviolet to the near-infrared spectral region. The reflectance measurements were supplied by the screen manufacturer and are traceable to NIST standards. The reflectance of the screen material is very constant throughout most of the optical wavelength range.

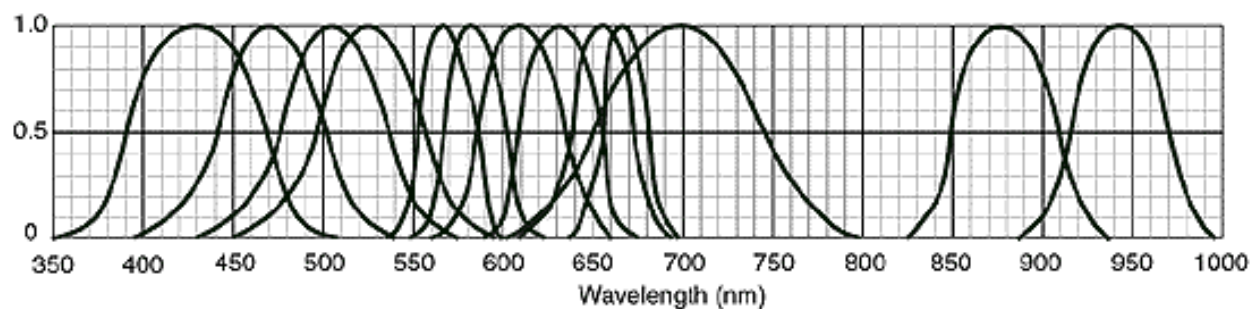


Fig. 3.— Spectral energy distributions of a sample of LEDs from Ledtronics, Inc. The figure is taken from the Ledtronics web page (<http://www.ledtronics.com>). Note that this is only a selection of the very wide range of colors available from this single manufacturer; many more are available from other vendors. Suitable combinations of these or other LEDs can provide almost any illumination spectrum.

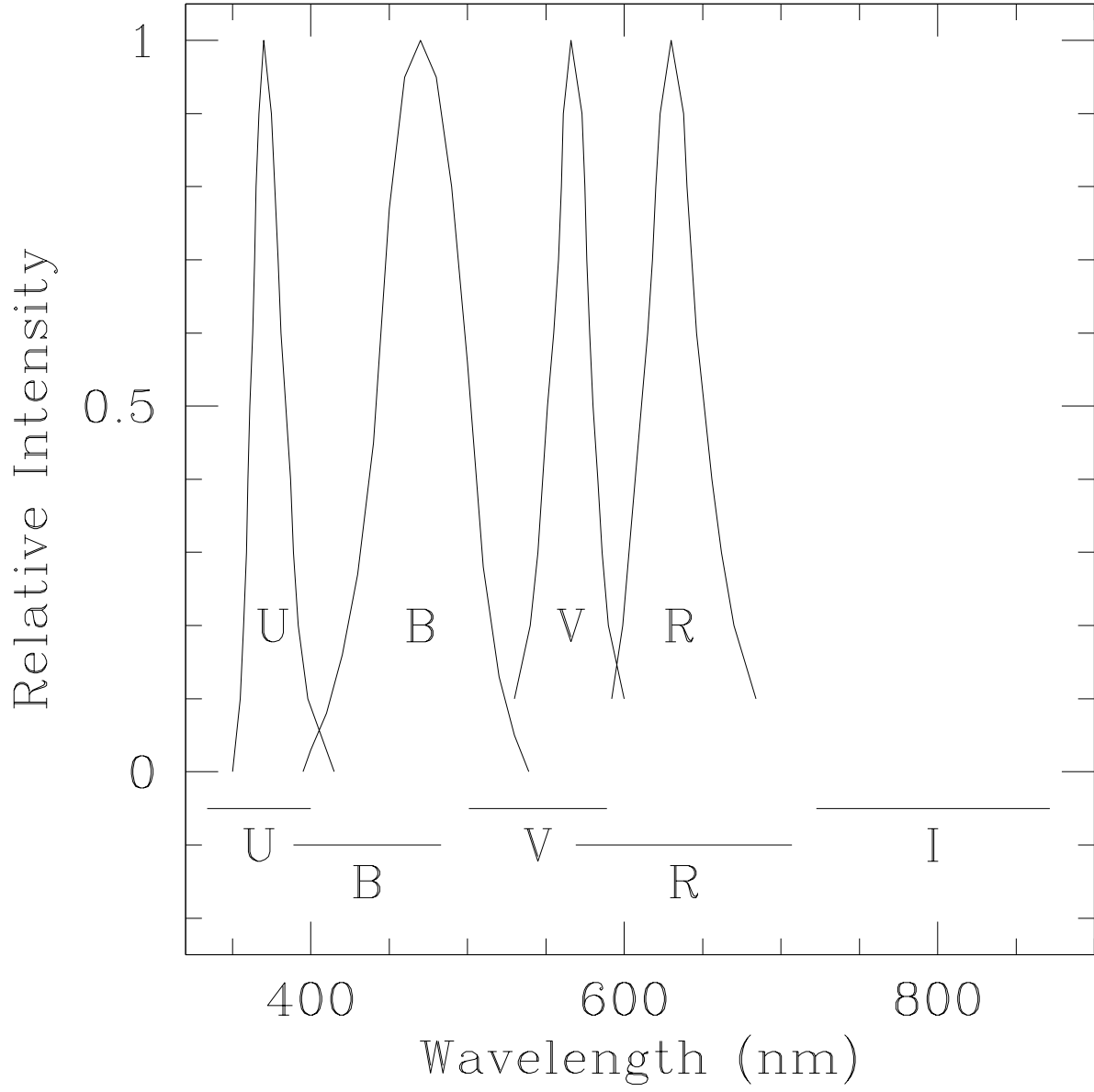


Fig. 4.— Spectral energy distributions of the UBVRI LEDs used in the MDM 1.3m flat field system. Typical optical filter bandpasses are shown across the bottom of the figure. These data are obtained from the manufacturers’ websites. The equivalent data for the I band LED were not available to us (the manufacturer specifies $\lambda_C \approx 810$ nm and $\Delta\lambda \approx 35$ nm, however).

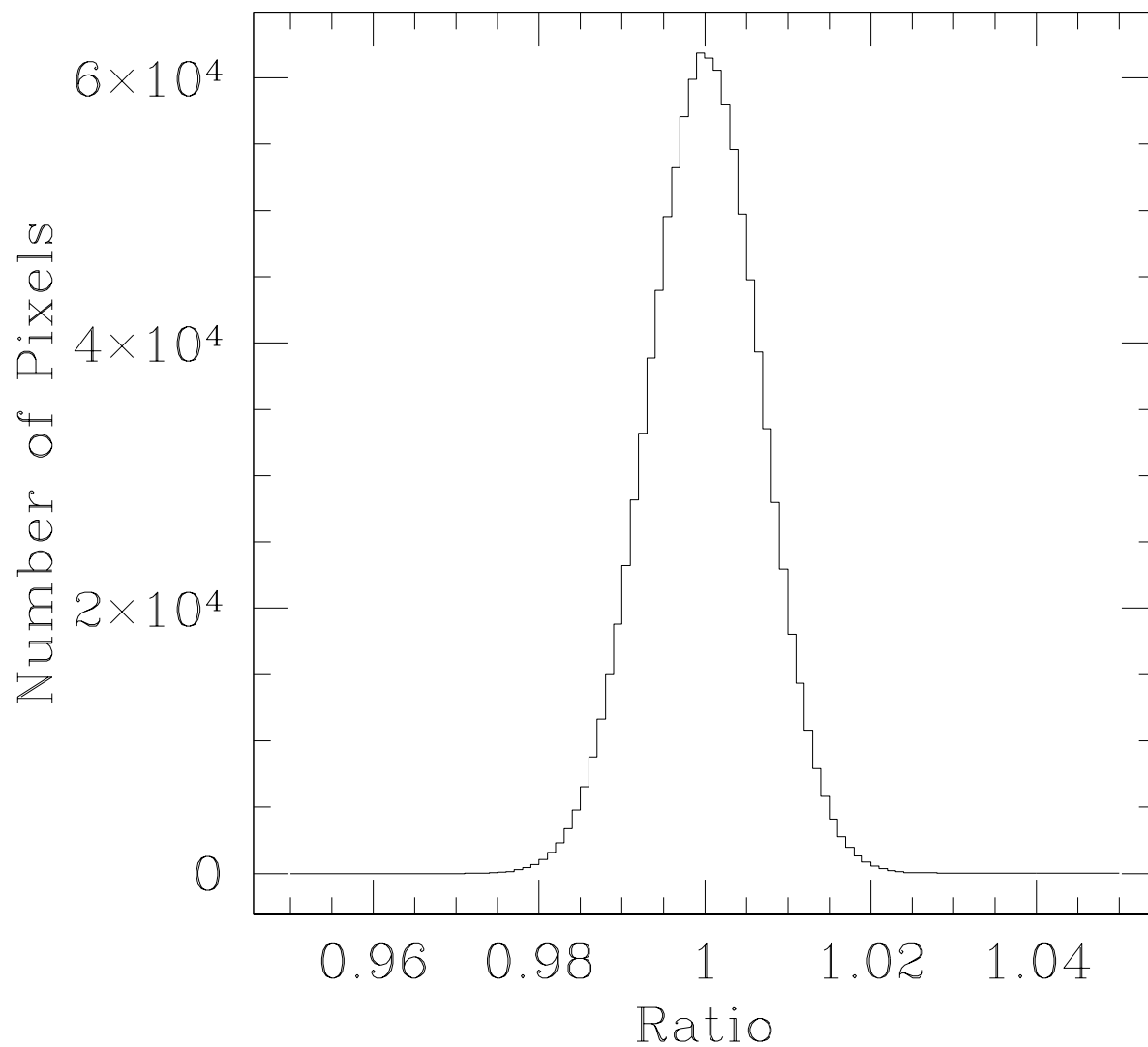


Fig. 5.— Histogram of values from the ratio of the twilight sky flat to the nighttime sky flat. The histogram is normalized to 1, and has a standard deviation of 0.7%

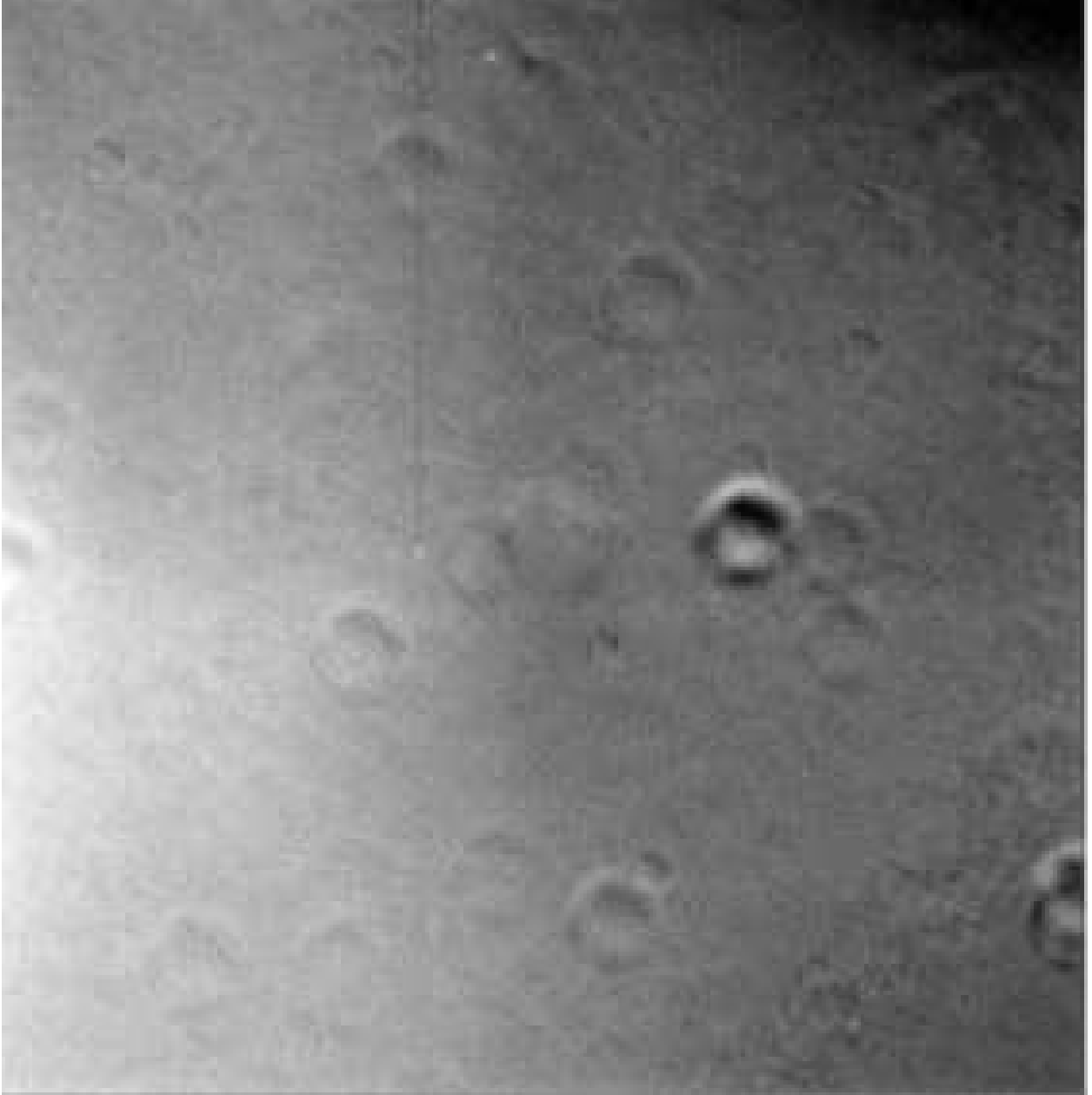


Fig. 6.— Ratio of a dome flat to the twilight sky flat. The grey scale used here ranges from roughly 0.97 (black) to 1.03 (white). The rings in the image are due to movement of dust particles on the optics of the system; the gradient across the image shows the different illumination pattern between the two flat fields.

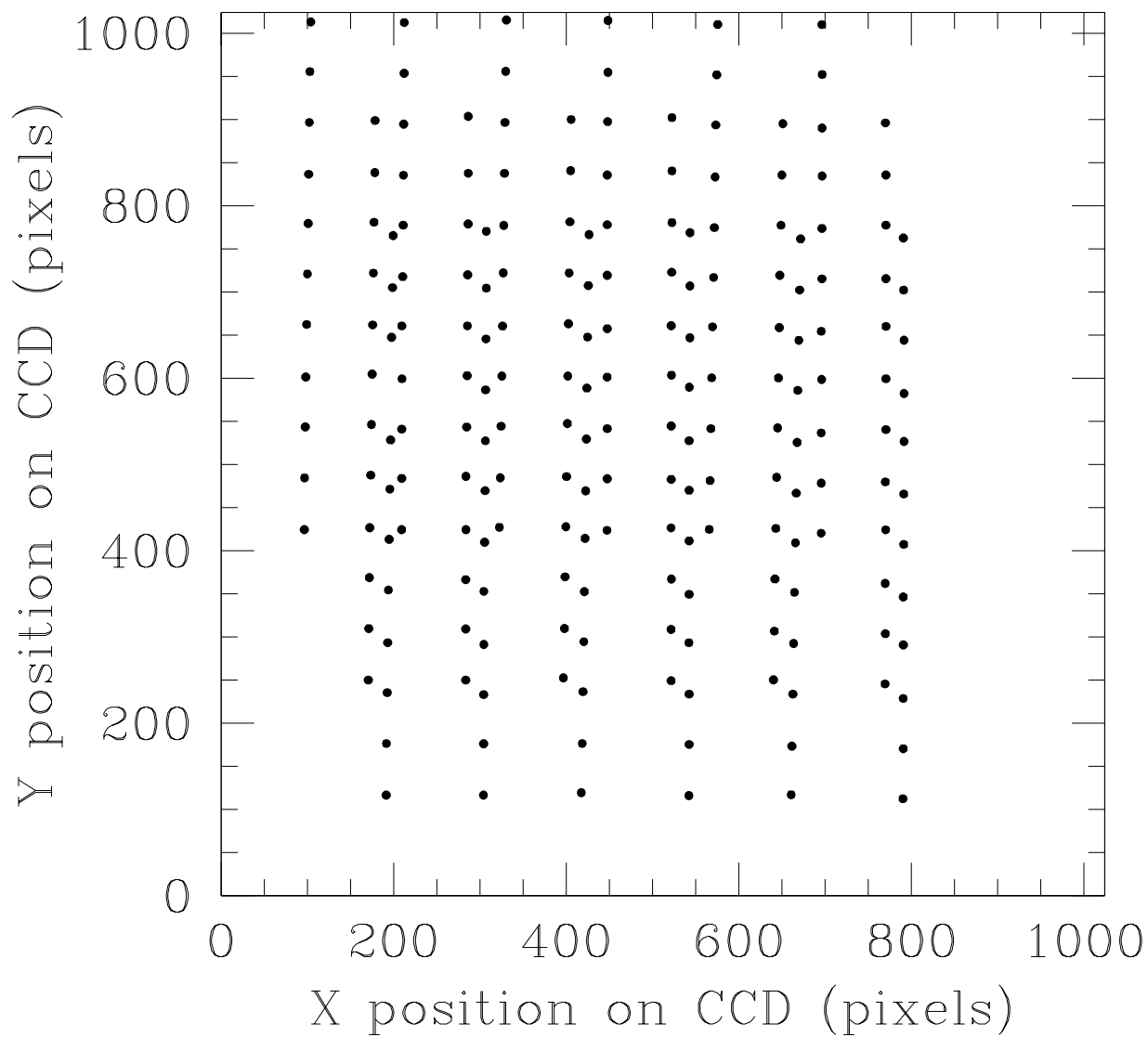


Fig. 7.— Positions of standard stars (SA112-275, SA112-250, and SA112-223; see Landolt 1992) used to test the various flat fields.

Table 1. LED Characteristics

Color	λ_C ^a (nm)	$\Delta\lambda$ ^b (nm)	V_F ^c (V)	I_F ^d (mA)	Viewing Angle (degrees)	Manufacturer	Part Number
U	370	23	3.9	10	110	LEDtronics	BP200CUV1K-250
B	470	65	3.8	20	125	LEDtronics	RL280TUB500-3.8
V	565	30	2.2	20	90	Panasonic	LN364GCP
R	630	40	2.1	20	90	Panasonic	LN864RCP
I	810	35	1.8	100	20	Roithner	ELD-810-525

^aWavelength of peak brightness of spectral energy distribution

^bFull-width at half-maximum of the spectral energy distribution of the LED

^cTypical voltage drop across LED due to current flowing in the forward direction

^dTypical forward current needed for optimal light output of LED

Table 2. Flat Field Comparisons: Standard Star Grid

	Sample standard deviation of photometric zero point after removal of gradient (mmag) ^a					
	no gradient	horizontal	vertical	radial from center	UL-LR	LL-UR
None	15.1	9.6	13.9	14.6	9.8	14.7
Twilight Sky	9.3	6.0	9.4	9.1	8.3	8.0
Dome Flat Position 1	6.6	6.2	6.5	6.6	6.2	6.5
Dome Flat Position 2	8.3	7.8	7.1	8.0	6.9	8.0
Dome Flat Position 3	13.2	10.1	10.7	13.1	13.0	6.2

^aStandard deviation of 205 measurements; see text for a description of gradient forms.